Structure determination of indium-induced Si(111)-In-4×1 surface by LEED Patterson inversion

J. Wang, Huasheng Wu,* Ricky So, Y. Liu, and M. H. Xie
Department of Physics and HKU-CAS Joint Lab on New Materials, The University of Hong Kong, Hong Kong, China

S. Y. Tong
Department of Physics and Materials Science, City University of Hong Kong, Hong Kong, China
(Received 24 March 2005; revised manuscript received 15 July 2005; published 19 December 2005)

A low-energy electron diffraction (LEED) Patterson function (PF) with multiple incident angles is used to determine the structure of the indium-induced Si(111)-4×1-In reconstructed surface. The experimental PF maps were compared with ones calculated by both single scattering and the tensor-LEED method according to various theoretical models so that one can pick out the right one. It was found that the model proposed by Bunk *et al.* is the best appropriate one, from which the induced PF maps are similar to the experimental ones. Further analysis of the PF spots obtained from the experimental PF maps directly generates the same model without any presupposition. It indicates that the multiple-incidence Patterson function is an effective method to determine the surface structure. Moreover, detailed atomic positions on surface were deduced from first-principles calculations and tensor-LEED *I-V* curve simulations. We also compared the results with those of previous investigations. Good agreement was found between them.

DOI: 10.1103/PhysRevB.72.245324 PACS number(s): 68.35.Bs

I. INTRODUCTION

The study of the reconstructions induced by a metal adsorbate on semiconductor surfaces has attracted considerable interest for many years. For the Si(111)-(7×7) surface, deposition of submonolayer metals causes various periodic surface structures upon annealing. Indium, especially, induces at least four reconstructions under different indium coverage: $(\sqrt{3}\times\sqrt{3})R30°$ at ~1/3 monolayer (ML), $(\sqrt{31}\times\sqrt{31})R9°$ at slightly higher coverage, 4×1 at 0.5–1 ML, and $(\sqrt{7}\times\sqrt{3})(1\times1-R30°)$. Among these four only the $(\sqrt{3}\times\sqrt{3})R30°$ phase has been extensively studied and its atomic structure has been well revealed.[1] However, details of other surface reconstructions remain unclear. Various techniques including reflection high-energy electron diffraction[2–4] (RHEED), low-energy electron diffraction[5–7] (LEED), scanning tunneling microscopy[8–10] (STM), Auger electron spectroscopy[4,6,11] (AES), impact collision ion scattering spectroscopy[12,13] (ICISS), transmission electron diffraction[14] (TED), and surface x-ray diffraction[11,15,16] (SXRD) have been used to investigate the 4×1 phase.

Some different structural models were proposed according to multifarious experimental results. First, Cornelison *et al.*[12] proposed an In overlayer structure, in which In atoms occupy the *H*3 and *T*4 sites from ICISS and STM data. Second, Nakamura, Anno, and Kono proposed a model with 1 ML In coverage from their Auger electron diffraction (AED), AES, and RHEED data.[4] Si atoms do not participate in the reconstruction in either of these two models. Third, based on TED results, Collazo-Davila *et al.*[14] gave another model which contains two In chains and a reconstructed double Si layer. The new observation of a 0.75 ML coverage of In from AES-LEED-STM data led Saranin *et al.*[6] to propose a π-bonded chain-stacking-fault model. More recently, Bunk *et al.*[16] used SXRD techniques to determine the structure of the 4×1 reconstruction and proposed a completely new model. This new SXRD model contains zigzag chains of silicon atoms on top of an unreconstructed silicon substrate and four indium atoms per unit cell located in two zigzag chains in the gap between the silicon chains. It was found that most of the previously published experimental data are consistent with this structural model. Serials of theoretical calculations subsequently strongly support this structural model.[17–19] In particular, Mizuno *et al.*[7] determined the detailed atomic arrangement of such a structure by using the tensor-LEED *I-V* curve simulation method. They found that the SXRD model has the lowest Pendry factor (R_p) among all the models they investigated. However, even if the best structure has a low-*R* factor, there is still no guarantee that another structure might not produce an even lower-*R* factor. Thus it should be interesting and necessary to further investigate the system of Si(111)-4×1-In surfaces by using other methods. The newly developed multiple-incidence Patterson inversion just provides such an appropriate tool.

Recently, an extended LEED Patterson function has been used to determine the vector positions of atoms relative to other atoms in the surface region.[20–22] Conventionally, Patterson inversion is an important tool in analyzing x-ray diffraction data due to the weak multiple scattering in x-ray diffraction which makes available the simple Fourier transform relationship between the diffracted amplitudes and the scattering potential.[23] It is generally known that the Patterson inversion gives a structure feature of the atom pairs in real space by performing a Fourier transform on the diffracted amplitudes, in which most of the useful information comes from single scattering. Unlike x-ray diffraction, LEED *I-V* spectra contain plentiful contributions from multiple scattering, which introduces an additional phase shift, resulting in strong noise or artifacts in the LEED Patterson function maps.[24] Sometimes, these artifacts make it nearly impossible

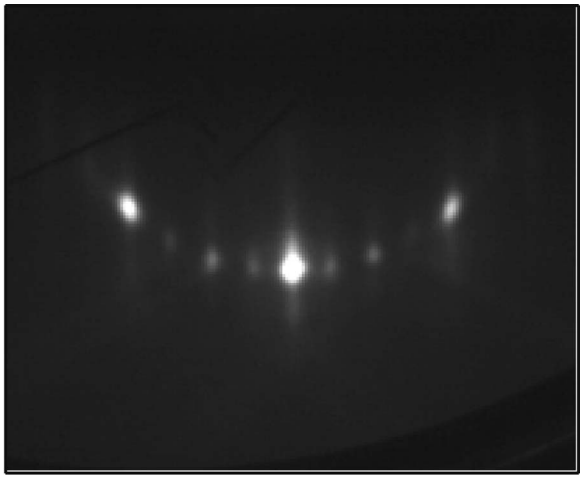

FIG. 1. *In situ* REED image for the Si(111)-4×1-In structure.

to obtain the surface structure from the conventional Patterson inversion. However, by including LEED *I-V* spectra at multiple incident directions and momentum transfers, such difficulties caused by multiple scattering in LEED can be overcome by multiple-incidence Patterson inversion.[20–22] Because LEED is very sensitive to surface atoms (down to several atomic layers), this method of extended LEED Patterson function can be used to select the right model from various ones and obtain a three-dimensional atomic structure.[21]

In this paper, we use the multiple-incident-angle LEED PF method to determine the structure of the Si(111)-4×1-In surface. The experimental PF maps were compared with ones calculated by using both single scattering and the tensor-LEED method according to certain theoretical models. It was found that the SXRD model proposed by Bunk *et al.* is the one that is most consistent with our data. The same model was also independently obtained from the experimental PF data directly by using our new computer program. Furthermore, detailed surface atomic positions were deduced from first-principles calculations and tensor-LEED *I-V* curve simulations. Good agreement was found in comparison with those of previous investigations.

II. EXPERIMENTS AND CALCULATIONS

The experiments were carried out in an ultrahigh-vacuum (UHV) system consisting of molecular beam evaporate (MBE), STM, LEED, atomic force microscopy (AFM), AES, and x-ray photoelectron spectroscopy (XPS). The Si (111) substrate, cut from a phosphorus-doped (1–10 Ω cm) wafer (Virginia Semiconductor) nominally with no miscut (less than 0.5°), was alternately rinsed in acetone and ethanol before being transferred into the UHV system. The substrate, after outgassed at 400 °C for 12 h, was resistively heated to 1150 °C for 20 s and slowly cooled down to room temperature to remove the oxide on the surface and produce a clean (7×7) surface. Indium was deposited from a Knudsen cell at ~0.05 ML/min on the sample at ~430 °C until a clear (4×1) reconstruction was observed. Figure 1 shows an *in situ* RHEED image for the obtained (4×1) reconstruction. The sample was then cooled down to room temperature and transferred to another μ-metal chamber to take LEED images.

An automated computer program was used to record LEED images at different incident angles in the energy range (20–230 eV) with constant electron momentum steps of 0.05 $Å^{-1}$. In the LEED experiments, a constant suppressor voltage of 4 V was used for collection of elastically scattered electrons. Fifteen incident directions were used. The polar angle θ was varied from 0° (normal) to 40° with a constant step of 10°. The azimuthal angle φ was varied from one mirror plane to its nearest-neighboring one (between 0 and 180°). The step of φ was varied with the value of θ in order to keep an approximately constant solid angle spanned by each direction in one irreducible region. The LEED *I-V* spectra were extracted from the acquired LEED images by using an automated procedure with optimization.[25]

To determine the atomic structure model, several sets of theoretical *I-V* curves with the same incident angles as those in the experiments were calculated according to different models by using both single scattering and the tensor-LEED package[26] to generate theoretical PF maps. Moreover, a newly developed MATLAB program package[27] was used to generate the surface structure directly from the recorded experimental PF spots' positions.

To determine accurate atomic positions based on the picked model, dynamical calculations, using the Barbieri–Van Hove automated tensor-LEED method,[26] were carried out to fit the experimental *I-V* curves. Nine phase shifts were used to represent atomic scattering. First-principles calculations were also performed in the framework of density functional theory using the Vienna *ab initio* simulation package.[28,29] In the calculations, ultrasoft scalar-relativistic pseudopotentials were used and the wave functions on a plane-wave basis were expanded up to an energy cutoff of 12 Ry. A supercell consisting of six atomic bilayers of Si, adlayers of Si and In, and a vacuum region of 20 Å was used.

III. RESULTS AND DISCUSSION

The as-grown film exhibits 4×1 LEED patterns with three identical domains with 120° between two adjacent domains. Two typical LEED patterns acquired at energies of 70 eV and 120 eV are shown in Figs. 2(a) and 2(b), respectively. A set of LEED *I-V* spectra for each domain were extracted from LEED images. A careful check of different spots' intensities and spectra shows that each domain has only one mirror plane. Figure 2(c) displays some LEED *I-V* spectra (solid lines) obtained from one set of data with a normal incident angle. One should notice that the intensities of integer spots have overlapped the contributions from three domains. To avoid artificial noise, those integer spots were excluded in the PF inversion process. Since those excluded spectra are just $\frac{1}{4}$ of the total ones, the final results should still be reasonable although some information arising from the substrate may be missing. However, this does not significantly affect our investigations of the surface reconstruction.

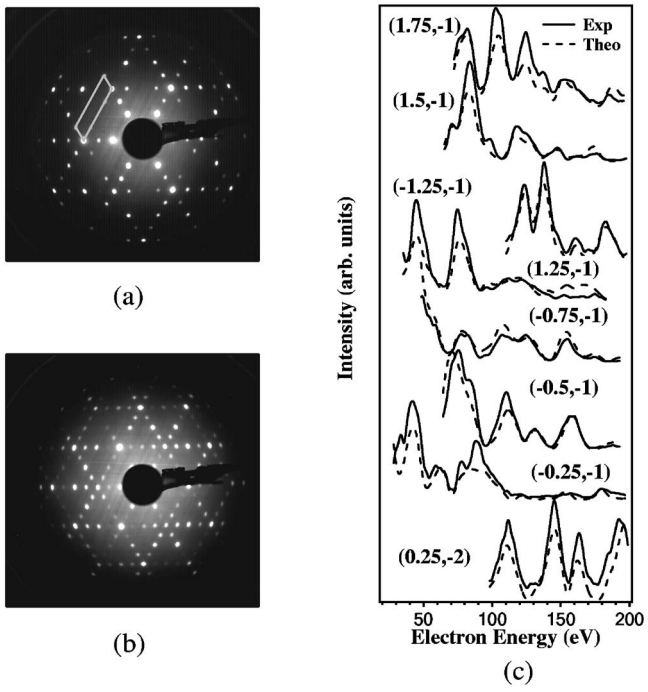

FIG. 2. (a) LEED pattern of the Si(111)-4×1-In structure at 70 eV. The 4×1 unit cell for one domain is outlined. (b) LEED pattern of the Si(111)-4×1-In structure at 120 eV. (c) Comparison between selected experimental and the best-fit theoretical *I-V* spectra of the Si(111)-4×1-In structure at normal incident angle.

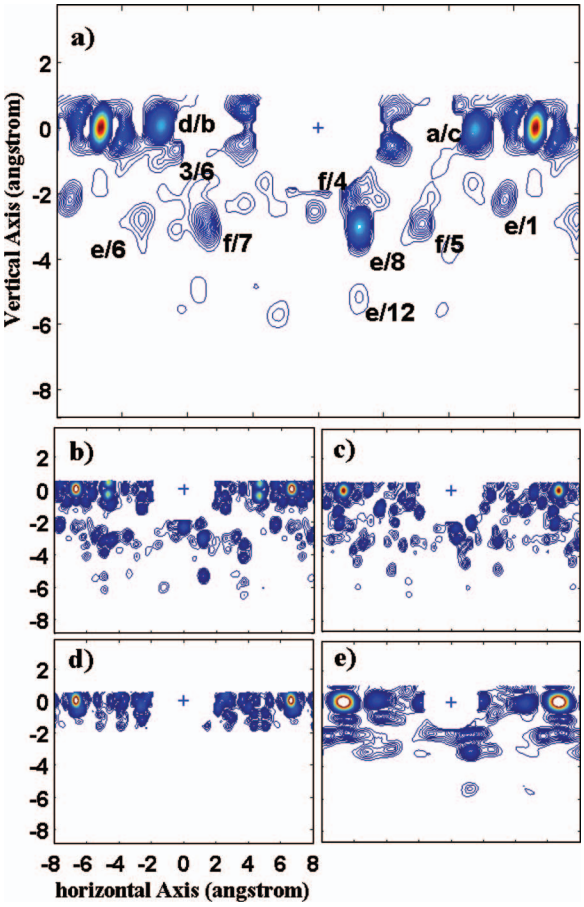

FIG. 3. (Color) LEED PF in the $(1\bar{1}0)$ plane from (a) the experimental LEED *I-V* spectra taken at 15 incident angles, (b) the simulated LEED *I-V* spectra for the SXRD model, (c) the simulated LEED *I-V* spectra for the STM model, (d) the simulated LEED *I-V* spectra for the TED model, and (e) the simulated LEED *I-V* spectra for the SXRD including multiple scattering. The numbers next to the spots in (a) correspond to the atomic pairs shown in Fig. 4.

Figure 3(a) displays the LEED PF map, viewed in the $(1\bar{1}0)$ cross-sectional plane, by inverting LEED *I-V* curves taken at 15 incident angles.[20,21] To suppress spurious noise near the origin, a sphere of radius 1.9 Å from the origin in the map was cut and set to zero. Thus those spots with a distance greater than 1.9 Å represent atomic pairs of the Si(111)-4×1-In structure. However, one should be careful in assigning spots to specific atomic pairs because some weak noise, resulting from disorder or defects on the imperfect surface, could be confused with real spots. In this presentation, the atomic structure model was obtained from a comparison of the experimental PF map with the simulated PF maps calculated with different models. Figures 3(b)–3(d) show the simulated PF maps from SXRD, STM, and TED models, respectively. To save computation time but still maintain the necessary structural features, the simulated PF maps were calculated using single scattering. Since single scattering already contains sufficient information about the surface structure, it is reasonable to use single scattering in the first step of simulation. Comparing (a) with (b), (c), and (d), one can immediately make a conclusion that the SXRD model was the best fit. To justify our simulation with single scattering, the PF map for the SXRD model is also calculated by using the tensor-LEED method, taking multiple scattering into account. Figure 3(e) displays the corresponding PF map, which is similar to that obtained from single-scattering calculations and our LEED experiments. Especially, atomic pairs of *f*-4, *e*-8, and *e*-12, contributed from the surface reconstruction and labeled in Fig. 3(a), are unique for SXRD model, which cannot be found in other models. These consistencies indicate that the SXRD model is the most possible atomic model for the Si(111)-4×1-In system in present experiments.

To completely figure out the structure, we recorded all spot positions appearing in the experimental PF maps and imported them into our program to generate the real-space structure of our sample. This program treats the substrate structure as known and puts one of the highest substrate atoms at the origin. Thus the overlayer atoms must be located at some PF spot positions above the origin. The program then uses a sophisticated algorithm to pick out the right PF spots to correspond with the overlayer atoms so that all experimental PF spots can be formed by interatomic pairs in the final structure, and inversely, all interatomic pairs in the final structure have their corresponding experimental PF spots. However, for the experimental data, noise and position shifts always exist in the PF maps. So we reduce a little bit the strictness of the criteria. A successful structure generated from the program should fulfill following two conditions: (a) The number of experimental PF spots that cannot be formed by interatomic pairs in the final structure should be as few as

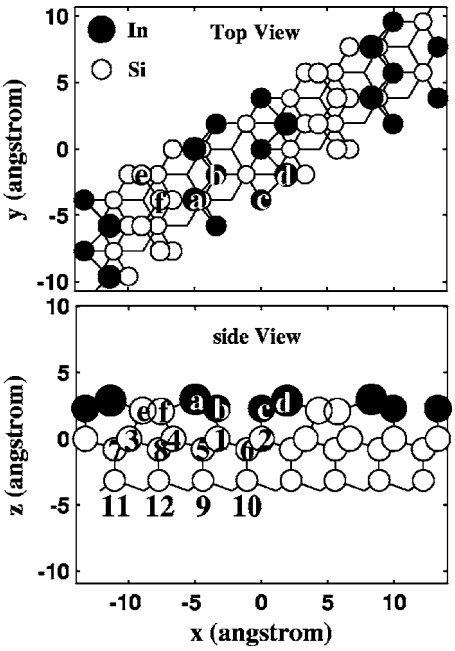

FIG. 4. Top (a) and side (b) views of the atomic structure for the Si(111)-4×1-In surface generated by our program.

possible, and (b) the number of nonmatching interatomic pairs in the final structure should be minimum.

Figures 4(a) and 4(b) exhibit the two-dimensional views on different planes of the structure model obtained from the program. On top of the silicon 1×1 substrate, one can find one Si zigzag chain per unit cell. Two indium zigzag chains are located in the gap between the adjacent silicon zigzag chains. Thus four indium and two silicon atoms form the surface of one unit cell. One can immediately determine that this structure is exactly the SXRD model. In other words, our experiments confirm that the atomic model of the Si(111)-4×1-In system is the SXRD model. It is worth pointing out that no preassumed model is needed to determine the atomic structure of the sample in our simulation. We just start from the position of PF spots recorded from the PF maps. The accuracy of the obtained atomic position from our method depends on the accuracy of the experimental data as well as the errors introduced by multiple-incidence Patterson inversion.

First-principles calculations and LEED *I-V* curve fitting with fully dynamical calculations were also performed to get refined atomic positions. Since the SXRD model has been decided to be the real one in the experiment of the LEED PF, we started from this model in our calculations. Sixteen symmetrically inequivalent beams were used for the tensor-LEED *I-V* curve simulation. The average Pendry *R* factor for the calculations is 0.161. Some simulated *I-V* curves from the fully dynamical calculations are shown in Fig. 2(c) by dashed lines, together with their corresponding experimental ones for comparison. The final atomic positions obtained by the two methods are listed in Table I. Good agreement between these two theoretical results is indicated. Table II shows the list of bond lengths obtained by different methods in different groups.[7,16] It was found that the results in the present work agree well with other experimental and theoretical studies.

TABLE I. Atomic positions obtained by first-principle and fully dynamical calculations. The axes of coordinates are shown in Fig. 4 (numbers given in Å).

	LEED simulations	First principles calculations
a (In)	(−5.03, 1.92, 0.00)	(−5.10, 1.88, 0.00)
b (In)	(−2.78, 0.00, 0.38)	(−2.84, −0.03, 0.39)
c (In)	(−0.39, 1.92, 0.43)	(−0.41, 1.90, 0.42)
d (In)	(1.89, 0.00, 0.02)	(1.83, −0.01, 0.00)
e (Si)	(−8.88, 0.00, 0.86)	(−8.97, −0.04, 0.79)
f (Si)	(−7.59, 1.92, 0.89)	(−7.59, 1.91, 0.82)
1 (Si)	(−3.25, 0.00, 3.03)	(−3.25, 0.00, 3.00)
2 (Si)	(0.00, 1.92, 3.07)	(0.11, 1.88, 3.03)
3 (Si)	(−9.89, 0.00, 3.11)	(−9.79, −0.03, 3.03)
4 (Si)	(−6.62, 1.92, 3.14)	(−6.66, 1.91, 3.06)
5 (Si)	(−4.38, 1.92, 3.79)	(−4.39, 1.91, 3.72)
6 (Si)	(−1.01, 0.00, 3.87)	(−1.07, 0.00, 3.85)
7 (Si)	(−11.05, 1.92, 3.78)	(−10.96, 1.88, 3.74)
8 (Si)	(−7.73, 0.00, 4.05)	(−7.66, −0.03, 3.96)
9 (Si)	(−4.39, 1.92, 6.16)	(−4.38, 1.91, 6.10)
10 (Si)	(−1.08, 0.00, 6.16)	(−1.06, 0.00, 6.18)
11 (Si)	(−11.01, 1.92, 6.14)	(−10.97, 1.88, 6.10)
12 (Si)	(−7.68, 0.00, 6.33)	(−7.66, 3.81, 6.26)

IV. CONCLUSION

A multiple-incidence LEED PF method was used to determine the structure of the Si(111)-4×1-In surface. The experimental PF maps were deduced from LEED *I-V* curves and compared with ones calculated by both single scattering and the tensor-LEED method according to different theoretical models. It was found that the SXRD model proposed by Bunk *et al.* is the best appropriate one which provides PF maps similar to the experimental map. Furthermore, the same surface structure as the SXRD model was directly ob-

TABLE II. List of bond lengths obtained in this work and previous experimental and theoretical studies (numbers given in Å).

Bond	LEED simulations (this work)	First-principles calculations (this work)	LEED (Ref. 7)	SXRD (Ref. 16)
In (*a*)-In (*b*)	3.08	2.98	2.91	2.99
In (*c*)-In (*d*)	3.02	2.97	3.00	2.97
In (*b*)-In (*c*)	3.07	3.10	3.24	3.15
In (*d*)-Si (*e*)	2.66	2.63	2.51	2.50
In (*a*)-Si (*f*)	2.71	2.62	2.59	2.62
In (*b*)-Si (1)	2.70	2.64	2.66	2.56
In (*c*)-Si (2)	2.67	2.66	2.67	2.74
Si (*e*)-Si (*f*)	2.31	2.36	2.43	2.40
Si (*e*)-Si (3)	2.47	2.38	2.33	2.54
Si (*f*)-Si (4)	2.47	2.42	2.40	2.55

tained by using a newly developed program. It indicates that the multiple-incident-angle Patterson function is an effective method to determine the surface structure. Moreover, first-principles calculations and LEED *I-V* curve fitting with tensor-LEED calculations were employed to generate the refined atomic positions. The obtained results agree well with those of previous investigations.

ACKNOWLEDGMENTS

The authors would like to thank Professor Gen Xu for his assistance in LEED dynamic calculations and Ho Win Kin for his technical assistance. Our work was supported by grants from Hong Kong's Research Grant Council (HK RGC Grant No. HKU 7095/01P)

*Corresponding author. Electronic address: hswu@hkusua.hku.hk

[1] V. G. Lifshits, A. A. Saranin, and A. V. Zotov, *Surface Phases on Silicon* (Wiley, New York, 1994).
[2] M. Kawaji, S. Baba, and A. Kinbara, Appl. Phys. Lett. **34**, 748 (1979).
[3] H. Hirayama, S. Baba, and A. Kinbara, Appl. Surf. Sci. **33/34**, 193 (1988).
[4] N. Nakamura, K. Anno, and S. Kono, Surf. Sci. **256**, 129 (1991).
[5] J. J. Lander and J. Morrison, Surf. Sci. **2**, 553 (1964).
[6] A. A. Saranin, E. A. Khramtsova, K. V. Ignatovich, V. G. Lifshits, T. Numata, O. Kubo, M. Katayama, I. Katayama, and K. Oura, Phys. Rev. B **55**, 5353 (1997).
[7] S. Mizuno, Y. O. Mizuno, and H. Tochihara, Phys. Rev. B **67**, 195410 (2003).
[8] S. Park, J. Nogami, and C. F. Quate, J. Microsc. **152**, 727 (1988).
[9] J. Nogami, S. I. Park, and C. F. Quate, Phys. Rev. B **36**, 6221 (1987).
[10] Y. Tanishiro, K. Kaneko, H. Minoda, K. Yagi, T. Sueyoshi, T. Sato, and M. Iwatsuki, Surf. Sci. **357/358**, 407 (1996).
[11] M. S. Finney, C. Norris, P. B. Howes, and E. Vlieg, Surf. Sci. **277**, 330 (1992).
[12] D. M. Cornelison, M. S. Worthington, and I. S. T. Tsong, Phys. Rev. B **43**, 4051 (1991).
[13] J. L. Stevens, M. S. Worthington, and I. S. T. Tsong, Phys. Rev. B **47**, 1453 (1993).
[14] C. Collazo-Davila, L. D. Marks, K. Nishii, and Y. Tanishiro, Surf. Rev. Lett. **4**, 65 (1997).
[15] M. S. Finney, C. Norris, P. B. Howes, M. A. James, J. E. Macdonald, A. D. Johnson, and E. Vlieg, Physica B **198**, 246 (1994).
[16] O. Bunk, G. Falkenberg, J. H. Zeysing, L. Lottermoser, R. L. Johnson, M. Nielsen, F. Berg-Rasmussen, J. Baker, and R. Feidenhans'l, Phys. Rev. B **59**, 12 228 (1999).
[17] R. H. Miwa and G. P. Srivastava, Surf. Sci. **473**, 123 (2001).
[18] J.-H. Cho, D.-H. Oh, K. S. Kim, and L. Kleinman, Phys. Rev. B **64**, 235302 (2001).
[19] J. Nakamura, S. Watanabe, and M. Aono, Phys. Rev. B **63**, 193307 (2001).
[20] Huasheng Wu and S. Y. Tong, Phys. Rev. Lett. **87**, 036101 (2001).
[21] Huasheng Wu, Shihong Xu, Simon Ma, W. P. Lau, M. H. Xie, and S. Y. Tong, Phys. Rev. Lett. **89**, 216101 (2002).
[22] S. H. Xu, Huasheng Wu, X. Q. Dai, W. P. Lau, L. X. Zheng, M. H. Xie, and S. Y. Tong, Phys. Rev. B **67**, 125409 (2003).
[23] A. L. Patterson, Phys. Rev. **46**, 372 (1934).
[24] D. L. Adams and Uzi Landman, Phys. Rev. B **15**, 3775 (1977).
[25] S. H. Xu, Huasheng Wu, Simon Ma, Win-kin Ho, and S. Y. Tong (unpublished).
[26] M. A. Van Hove, W. Moritz, H. Over, P. J. Rous, A. Wander, A. Barbieri, N. Materer, U. Starke, and G. A. Somorjai, Surf. Sci. Rep. **19**, 191 (1993).
[27] Huasheng Wu *et al.* (unpublished).
[28] G. Kresse and J. Furthmuller, Phys. Rev. B **47**, R558 (1993); **49**, 14251 (1994); **54**, 11169 (1996); G. Kresse and D. Joubert, *ibid.* **59**, 1758 (1999).
[29] G. Kresse and J. Hafner, J. Phys.: Condens. Matter **6**, 8245 (1994).